

Can we speed up 3D scanning? A cognitive and geometric analysis

Karthikeyan Vaiapury

Balamuralidhar Purushothaman

Arpan Pal

Swapna Agarwal

Brojeshwar Bhowmick
Embedded systems and Robotics
TCS Research and Innovation
India

(karthikeyan.vaiapury, balamurali.p, arpan.pal, agarwal.swapna, b.bhowmick)@tcs.com

Abstract

The paper propose a cognitive inspired change detection method for the detection and localization of shape variations on point clouds. A well defined pipeline is introduced by proposing a coarse to fine approach: i) shape segmentation, ii) fine segment registration using attention blocks. Shape segmentation is obtained using covariance based method and fine segment registration is carried out using gravitational registration algorithm. In particular the introduction of this partition-based approach using visual attention mechanism improves the speed of deformation detection and localization. Some results are shown on synthetic data of house and aircraft models. Experimental results shows that this simple yet effective approach designed with an eye to scalability can detect and localize the deformation in a faster manner. A real world car use case is also presented with some preliminary promising results useful for auditing and insurance claim tasks.

1. Introduction and Review

In the modern scientific era, change detection demands real or at least near real time and good precision for many real world applications including quality inspections maintenance, repair and overhaul (MRO), view planning for shooting scene footage for smart robotics or drone application, urban planning for smart cities, surgical operations in medical domains etc. The paper tries to solve a fundamental problem in 3D scanning: shape matching and deformation localization using cognitive aspects. From a generic perspective, a plethora of survey of 2D and 3D change detection is provided in [9] and the need of innovative basic research in change detection mechanism is emphasized. There are methods [12] [14] [11] which uses point clouds from 3D laser range sensors for detecting change in position of existing objects, or detecting a new object in the scene.

Existing 3D change detection algorithm [14] [8] [5] in general comprises the common steps - registration between two point clouds and thresholding the distance between the vertices of the point clouds to detect significant changes. The challenges are mainly due to registration errors, irregularities in the point cloud, density difference between source and target point clouds, sensor noise, sensitivity of the detection method to small changes etc. Point clouds representing large data typically contain very high number of points and hence an algorithmic trade-off is required between sensitivity to small changes and computational complexity. For example, change detection on building sites or inside facilities, using a ground-based laser scanning device[5], there is a lower emphasis on precision of measured displacement compared to speed of the data analysis. To handle computational complexity trade-off, in [2], a new OBB oriented bounding box regional area descriptor is proposed which is quite useful for 3D point cloud registration when no coordinate reference exist. The precision of change detection depends on precision and distribution of common points of source and target point cloud using which conversion coefficients can be obtained [7]. Recently, a method for robust change detection using implicit surface defined by growing least square reconstruction is proposed in [4] compared to standard proximity measure approach. In [12], point clouds are modeled by a mixture of Gaussian which require high computation due to the energy minimization algorithms and require the number of Gaussians in advance. Another approach [14] applies a 3D bounding box to registered point clouds and models the global density function by summing local density functions fitted to each point. Changes in the point clouds are expressed as a boolean operation over the global density functions after thresholding. However, in this method the efficiency decreases when the surfaces are not closed.

The need for cognitive principles and increased interest in biologically inspired systems is well appreciated in research community. Bridewell has proposed a change detection ar-

chitecture ARCADIA using color blindness phenomenon [1]. Generic pipeline of cognitive change detection (ARCADIA) include a) bottom up feature computation, b) Iconic Memory, c) Fixation generators, d) Early binding, e) Identity, f) Visual short term memory (vSTM), g) change detection. ARCADIA's fixation generators include both bottom up and top down factors, identity component tracks equality between old and new object representations. This component compares focused objects to those reported by vSTM and posts an interlingua element that specifies an identity relationship between the new object and the object from vSTM. The comparison is based on size and location of the new object against the last known size and location available in vSTM. In domain specific problems, the size, location information of the components are available in CATIA or XML formats [13]. Precisely, the dimensions and pose information including rotation and translation are available aprior. The sample XML representation is provided in Fig. 1. The model knowledge includes various parameters such as dimensions, length, height, width, rotation, translation can be embedded in a tree like structure which is parsed using XML reader [13]. Recently, a study on attention driven cognitive vision architecture is also made on a remote sensing case study [3]. First time to the best of our knowledge, we propose a framework based on combination of OBB-AB and gravitational based fitting for 3D shape analysis which can be used for production audit in assisting qualitative assessment for manufacturing and insurance process in automotive domain. It will reduce the processing time of some of the manual process used in insurance claim process. This technology is useful for examining the healthiness of sub parts using checklist and domain model knowledge. The key contributions of our paper are:

- we propose a novel bi-level framework where we use covariance based shape segmentation followed by gravitational fitting and MLS matching.
- The method works only on saliency segment reducing the computational complexity from $O(n)$ to $O(n/k)$ where $k = 2, 4, 8$,
- the method works even when there is density variation between source and target point clouds and capable of capturing even miniature changes.

2. Proposed solution methodology

The proposed solution consists of A) Covariance based shape segmentation, B) Finer registration using gravitational based fitting and attention. The framework can be used for examining the subparts of any installation using model knowledge which are described below.

```
<?xml version="1.0" encoding="utf-8" ?>
- <shapes unit="mm">
- <shape type="CALIBRATION" name="c5" kind="component">
  <dimensions x="8" y="3" z="10" />
  <color r="0.0" g="0.0" b="0.0" />
  <transparency value="0.0" />
  <translationPt x="10" y="40" z="0" />
  <XVector x="1.0000" y="0.0000" z="0.0000" />
  <YVector x="0.0000" y="1.0000" z="0.0000" />
  <ZVector x="0.0000" y="0.0000" z="1.0000" />
</shape>
- <shape type="CUBE" name="c1" kind="component">
  <dimensions x="30" y="0" z="0" />
  <color r="0.0" g="0.0" b="1.0" />
  <transparency value="0.0" />
  <translationPt x="25" y="135" z="60" />
  <XVector x="1" y="0" z="0" />
  <YVector x="0" y="1" z="0" />
  <ZVector x="0" y="0" z="1" />
</shape>
- <shape type="RECTANGULARPRISM" name="c2" kind="component">
  <dimensions x="30" y="90" z="15" />
  <color r="0.0" g="1.0" b="0.0" />
  <transparency value="0.0" />
  <translationPt x="25" y="135" z="7.5" />
  <XVector x="1.0000" y="0.0000" z="0.0000" />
  <YVector x="0.0000" y="1.0000" z="0.0000" />
  <ZVector x="0.0000" y="0.0000" z="1.0000" />
</shape>
```

Figure 1. XML format of the components [13]

2.1. Covariance based Shape segmentation into sub-blocks

The orientations of OBB is calculated for the given point cloud under scanning based on covariance-based method [2].

Given p and p' the number of vertices in a point cloud in the form $X = (a \ b \ c)$, the method project the points in point cloud to eigen vectors to determine the three directions of OBB by calculating the distance between the farthest and nearest projected points in each eigen vector.

The OBB is represented by $c = (a_c, b_c, c_c)$ and cc_1, cc_2, cc_3 which can be calculated using following equations.

$$a_c = \mu_a + \nu_{11}a'_{min} + \nu_{21}b'_{min} + \nu_{31}c'_{min} \quad (1)$$

$$b_c = \mu_b + \nu_{12}a'_{min} + \nu_{22}b'_{min} + \nu_{32}c'_{min} \quad (2)$$

$$c_c = \mu_c + \nu_{13}a'_{min} + \nu_{23}b'_{min} + \nu_{33}c'_{min} \quad (3)$$

$$cc_1 = (a'_{max} - a'_{min})v_1 \quad (4)$$

$$cc_2 = (b'_{max} - b'_{min})v_2 \quad (5)$$

$$cc_3 = (c'_{max} - c'_{min})v_3 \quad (6)$$

where $a'_{min} = \min\{a'_j, \forall j = 1, 2, \dots, p\}$; $b'_{min} = \min\{b'_j, \forall j = 1, 2, \dots, p\}$; $c'_{min} = \min\{c'_j, \forall j = 1, 2, \dots, p\}$; $a'_{max} = \max\{a'_j, \forall j = 1, 2, \dots, p\}$; $b'_{max} = \max\{b'_j, \forall j = 1, 2, \dots, p\}$; $c'_{max} = \max\{c'_j, \forall j = 1, 2, \dots, p\}$

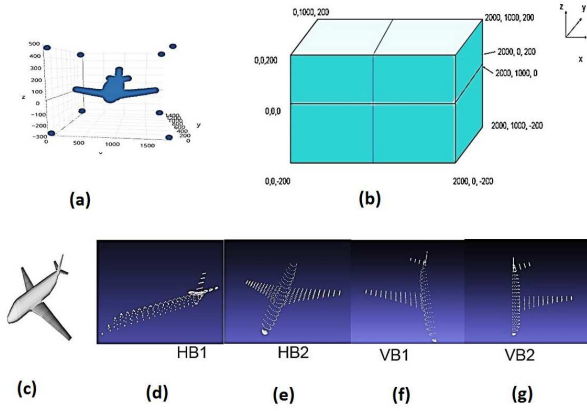


Figure 2. top: a) obb corners, b) coordinate system below: c) aircraft model d) horizontal bi-block1 partitioned cloud HB₁ e) horizontal bi-block 2 partitioned cloud HB₂ f) vertical bi-block 1 partitioned cloud VB₁ g) vertical bi-block 2 partitioned cloud VB₂(better viewed in color).

$1, 2 \dots p\}$; $c'_{max} = \max\{c'_j, \forall j = 1, 2 \dots p\}$ a'_j, b'_j, c'_j is calculated as

$$a'_j = \nu_{11}(a_j - \mu_a) + \nu_{12}(b_j - \mu_b) + \nu_{13}(c_j - \mu_c) \quad (7)$$

$$b'_j = \nu_{21}(a_j - \mu_a) + \nu_{22}(b_j - \mu_b) + \nu_{23}(c_j - \mu_c) \quad (8)$$

$$c'_j = \nu_{31}(a_j - \mu_a) + \nu_{32}(b_j - \mu_b) + \nu_{33}(c_j - \mu_c) \quad (9)$$

ν_1, ν_2, ν_3 are eigen vectors calculated from covariance matrix from M, M' as $cov^X = \frac{1}{p} X(X)^T$

By using the co-ordinate system knowledge, we chunk the OBB into level like horizontal bi block, vertical bi block, quad block and oct block. Fig. 2 shows the OBB corners extracted for aircraft dataset, associated partitioned blocks based on the values from table.2.

2.2. Fine registration using visual attention

For alignment of the segments in each salient pair, we follow the gravitational approach based registration (GR) proposed in [6]. According to this approach, each particle of an abject attracts each other particle of the other object. This force of attraction is proportional to the multiplication of the mass of the two particles involved and the distance between the two particles involved. This force of attraction helps in the alignment of the two objects. In our case, given the pair of salient 3D segments S_A and S_B , the gravitational force applied on each point of S_B by all the points of S_A is estimated as

$$F_{Bi} = -Gm_{Bi} \sum_{j=1}^N \frac{m_{Ai}}{\|r_{Bi} - r_{Aj}\|} n_{ij} \quad (10)$$

Block	x_{min}	x_{max}	y_{min}	y_{max}	z_{min}	z_{max}
HB ₁	0	2000	0	1000	0	200
HB ₂	0	2000	0	1000	-200	0
VB ₁	0	1000	0	1000	-200	200
VB ₂	1000	2000	0	100	-200	200
QB ₁	0	1000	0	1000	0	200
QB ₂	1000	2000	0	1000	0	200
QB ₃	0	1000	0	1000	-200	0
QB ₄	1000	2000	0	1000	-200	0
OB ₁	0	1000	0	500	0	200
OB ₂	0	1000	655	1000	0	200
OB ₃	1000	2000	0	655	0	200
OB ₄	1000	2000	655	1200	0	200
OB ₅	0	1000	0	655	-200	0
OB ₆	0	1000	655	1200	-200	0
OB ₇	1000	2000	0	655	-200	0
OB ₈	1000	2000	655	1200	-200	0

Table 1. Partition block table sample H-Horizontal, V-Vertical, Q-Quad, O-Octo B-Block.

Objectparts	H_{B1}	H_{B2}	V_{B1}	V_{B2}
AC Elevator				ν
AC Fuselage	ν			
AC Left wing			ν	
AC Right wing				ν
AC Rudder		ν		
AC Stabilizer		ν		ν
Car Logo	ν			
Car Licenseplate	ν			
Car Bumper	ν			
Car fender	ν			
Car hoods	ν			
Car tailgatestrunk		ν		
Car doorleft			ν	
Car doorright				ν
Car mirrorleft			ν	
Car mirrorright				ν
Car tyreleft			ν	
Car tyreright				ν

Table 2. Attention block. AC-Aircraft

where, m_H and r_H represent the mass and the absolute coordinate of the point cloud vertex H ($H \in \{S_{Ai}, S_{Bj}\}$). G is the gravitational constant and the unit vector in the direction of force is represented by n_{ij} .

The total gravitational force applied on S_A is the summation of the force applied on individual vertex of S_B . The segment S_B , as a rigid body, aligns towards S_A under the force F_B in a number of iterations using the following equation.

$$S_A(t+1) = sS_A(t)R + T, \quad (11)$$

where s , R and T represent scale, rotation and translation respectively of S_A as obtained due to the gravitational force. The index t is used to represent the iteration number.

The source and the target point clouds A and B after sub-sampling are divided into voxels of size $K \times K \times K$. 3D points in each voxel are processed to generate an approximate surface using moving least square [10] which reconstructs a surface from a set of vertices using weighted least square.

In each voxel, let there be P vertices where $P = \{p_i\}$ and $p_i \in \mathbb{R}^3$. Let the function f be a set of distances from the P vertices to a local reference plane such that, $f(p_i) = f_i$, where $f_i \in \mathbb{R}$. Then, using a polynomial function $g(p_i)$, the surface can be estimated at a position $q \in \mathbb{R}^3$ by minimizing the weighted least square equation as follows

$$\sum_{i=1}^P (g(p_i) - f_i)^2 \theta(\|q - p_i\|) \quad (12)$$

Where θ represents the smooth monotonically decreasing weight in the system and can be defined as $\theta(s) = e^{-\frac{s^2}{\sigma^2}}$ σ is a constant term which represents the spacing between neighboring voxels. In our experiment, we compute a sixth order polynomial fitting for generating surface. The coefficients of the polynomial $g(p_i)$ provides surface information of a local region in point cloud and therefore can be used to detect change. c_A and c_B are the polynomial coefficients fitted in a voxel of point cloud A and B respectively and are used as feature vectors to describe the change in the point cloud. For every vertex of the voxel in A, a boolean attribute distort is defined as in following equation which indicates if the vertex has undergone change in B. For every feature vector of A, the nearest neighbor feature vector of B is selected from the kd-tree and if the distance between the input feature vector and searched feature vector $d(c_A, c_B)$ is negligible, then the vertex of the input feature vector is said to be undistorted. Otherwise, it has undergone change in B.

$$distort = 0 \text{ if } d(c_A, c_B) < \delta; 1 \text{ otherwise} \quad (13)$$

Where, δ is a threshold.

3. Results and discussion

The proposed change detection system is tested on HP Envy 6 Notebook AMD A6-4455M APU with Radeon HD Graphics 6 GB RAM. In order to demonstrate the utility of the proposed methodology, we created synthesized data sets of house and aircraft model. For instance, if a reference 3D model of an aircraft is given and in another scan of the aircraft is deformed in one of its wing, then detecting and

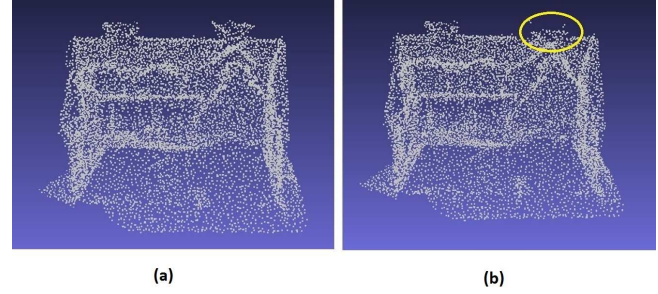


Figure 3. House a) normal vs. b) deformed: Ground truth(better viewed in color).

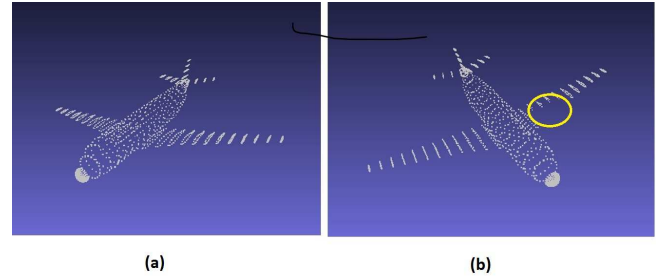


Figure 4. Aircraft a) normal vs. b) deformed: Ground truth(better viewed in color).

estimating that change can lead to fast inspection and quality control. In another scenario, a model of a building is given and a damaged roof segment is presented for change estimation (refer Fig.3 and 4).

For the former model, deformation is done using the elliptic deformation technique i.e, using parametric function $g(x, y, z)$ such as elliptic paraboloid and the later model by the deletion of selected vertices. The total number of source and target vertices of house and aircraft dataset are (9577,9525) and (1335,1291) respectively. The source and the target point cloud are processed using the proposed pipeline to detect the change. The percentage of deformation level (PDL) is quantified by the ratio between estimated number of deformed vertices to the number of deformed vertices in ground truth. The proposed system is capable of correctly identifying the deformation in rigid objects with geometrical structures such as house and aircraft dataset (refer Fig.8 and 9). The deformation in chimney like structure in house and deformation in aircraft wing is detected and localized. We also run the experiment for the whole point cloud without using OBB-AB and purely based on GR and MLS approach (refer Fig.6 and 7). PDL is 82.8% for house and 100% for aircraft same as with OBB-AB based GR and MLS approach. By effectively identifying the salient pairs, the processing of whole point cloud is alleviated at the cost of OBB-AB approach while achieving the same result. The

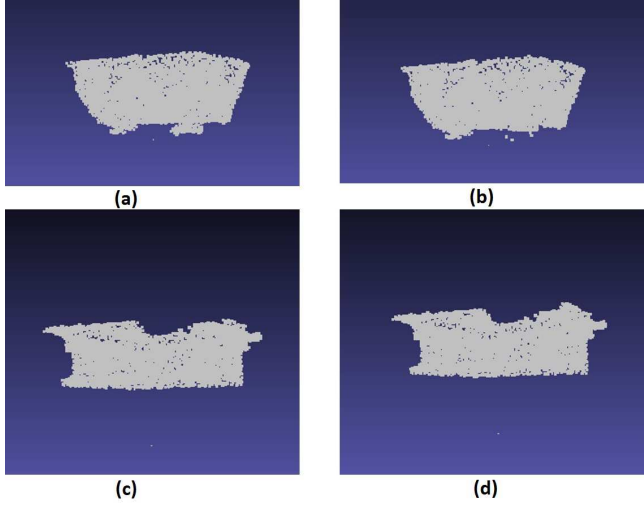


Figure 5. OBB segment house HB₁(top) HB₂(bottom) a,c-normal, b,d-deformed (better viewed in color)

computational complexity is reduced by k times where

$$k = \frac{\text{number of segmented vertices}}{\text{total number of vertices in point cloud}} \quad (14)$$

. In the house and aircraft data set shown, k is 2. Though the detected changes due to deformation based on elliptic paraboloid are visible, the results can be still improved. Further, we manually introduced some errors that is distributed across the segments to check the reliability of the algorithm. As shown in Fig. 10, the system is able to capture even the miniature intrinsic details, handling the perturbations and correctly detect the changes along cockpit and rudder. Finally, we showcase the 3D model of car in which the missing logo is detected (refer Fig. 11). The corresponding camera views of the 3D model is shown in Fig. 12. By mapping the semantic to attention block, view planning can be accomplished. For example, in this case, only rear part of the scene is processed which could be useful for the automation of insurance claim processes/auditing using smart camera vision with robotics or drones.

4. Conclusion

In this paper, we proposed a cognitive inspired change detection for detecting and localizing deformations in texture-less point clouds. At first level, we have shown how obb is used to partition point clouds and demonstrated how to estimate the deformation. The utility is tested on synthetic aircraft and house data sets. Experimental results shows that this simple yet effective approach detect and localize the deformation. A real world car use case is also presented with some preliminary promising results useful for auditing and insurance claim tasks.

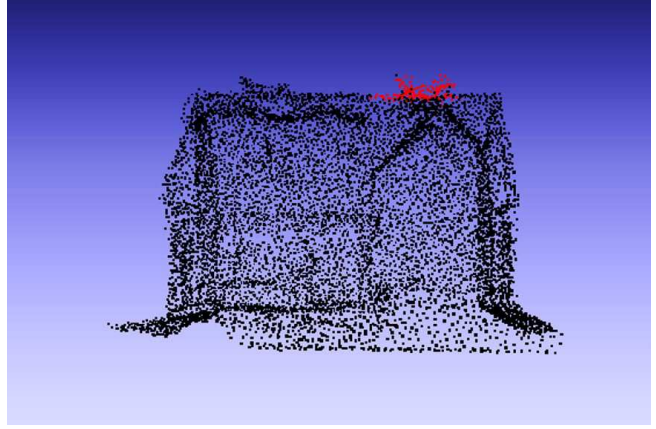


Figure 6. Actual detected result: Localization of deformation using method GR [6] +MLS (house)(better viewed in color).

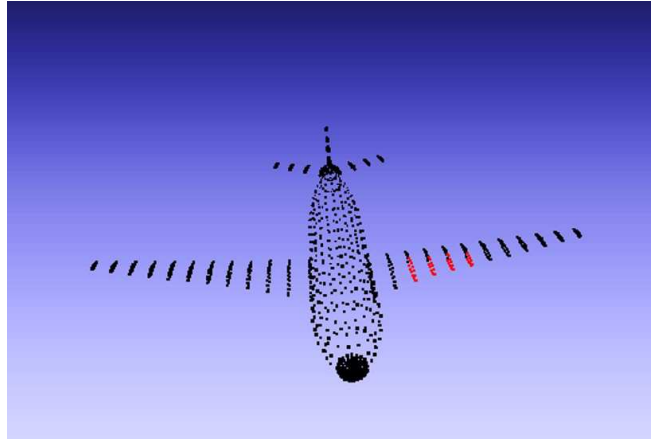


Figure 7. Actual detected result: Localization of deformation using method GR [6] +MLS (aircraft)(better viewed in color).

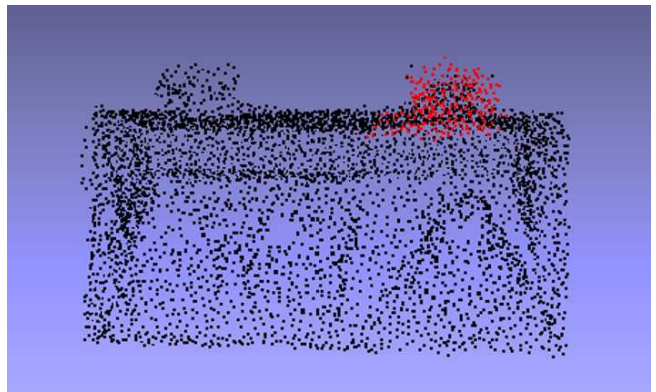


Figure 8. Actual detected result: Localization of deformation using method OBB-AB+GR [6] +MLS (house)(better viewed in color).



Figure 11. 3D change detection of car.



Figure 12. Corresponding camera views of the car.

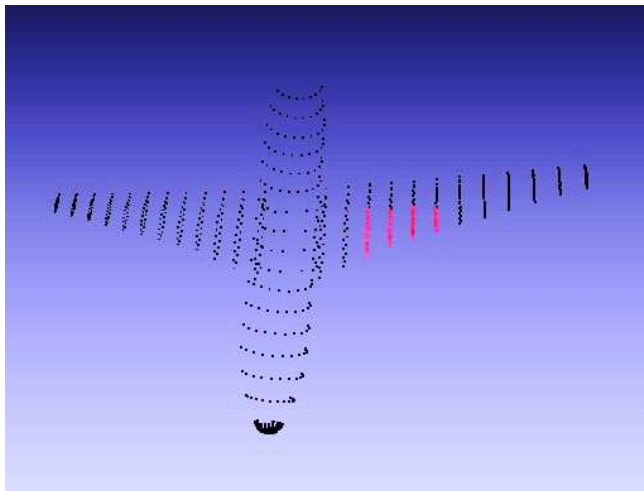


Figure 9. Actual detected result: Localization of deformation using method OBB-AB+GR [6] +MLS (aircraft)(better viewed in color).

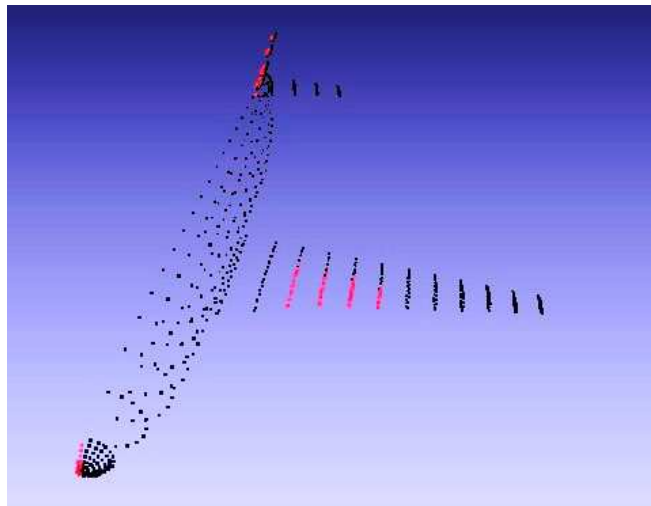


Figure 10. Actual detected result: Localization of deformation using method OBB-AB+GR [6] +MLS(aircraft)(better viewed in color).

References

- [1] W. Bridewell and P. Bello. Incremental object perception in an attention-driven cognitive architecture. In *37th Annual Meeting of the Cognitive Science Society*, 2015.
- [2] L. Chen, D. Hoang, H. Lin, and T. Nguyen. Innovative methodology for multi-view point cloud registration in robotic 3d object scanning and reconstruction. In *In Appl. Sci*, 2016.
- [3] S. Deshpande, A. Sowmya, P. Yadav, S. Ladha, P. Verma, K. Vaiapury, J. Gubbi, and P. Balamuralidhar. Cogvis: Attention-driven cognitive architecture for visual change detection. In *Proceedings of the Symposium on Applied Computing*, SAC '17, pages 151–154, New York, NY, USA, 2017. ACM.
- [4] P. Gianpaola, C. Paola, B. Tamy, and S. Roberto. Detection of geometric temporal changes in point clouds. *Computer Graphics Forum*, 35(6):33–45, 2016.
- [5] D. Girardeau-Montaut, M. Roux, R. Marc, and G. Thibault. Change detection on points cloud data acquired with a ground laser scanner. *International Archives of Photogrammetry, Remote Sensing and Spatial Information Sciences*, 36(part 3):W19, 2005.
- [6] V. Golyanik, S. Aziz Ali, and D. Stricker. Gravitational approach for point set registration. In *In Proceedings of the*

IEEE Conference on Computer Vision and Pattern Recognition, page 58025810, 2016.

- [7] M. Hou, S. Li, L. Jiang, Y. Wu, Y. Hu, S. Yang, and X. Zhang. A new method of gold foil damage detection in stone carving relics based on multitemporal 3d lidar point clouds. *ISPRS International Journal of Geoinformation*, 5, 2016.
- [8] Z. Kang and Z. Lu. The change detection of building models using epochs of terrestrial point clouds. In *Multi-Platform/Multi-Sensor Remote Sensing and Mapping (M2RSM), 2011 International Workshop on*, pages 1–6. IEEE, 2011.
- [9] K. Konstantinos. Recent advances on 2d and 3d change detection in urban environments from remote sensing data. *Springer Chapter: Computational approaches for urban environments, Geotechnologies and the environment*, 13:237–272, 2014.
- [10] D. Levin. The approximation power of moving least-squares. In *Mathematics of Computation of the American Mathematical Society*, page 15171531, 1998.
- [11] O. Monserrat and M. Crosetto. Deformation measurement using terrestrial laser scanning data and least squares 3d surface matching. *ISPRS Journal of Photogrammetry and Remote Sensing*, 63(1):142–154, 2008.
- [12] P. Núñez, P. Drews, A. Bandera, R. Rocha, M. Campos, and J. Dias. Change detection in 3d environments based on gaussian mixture model and robust structural matching for autonomous robotic applications. In *Intelligent Robots and Systems (IROS), 2010 IEEE/RSJ International Conference on*, pages 2633–2638. IEEE, 2010.
- [13] K. Vaiapury, A. Aksay, X. Lin, E. Izquierdo, and C. Papadopoulos. A vision based audit method and tool that compares a systems installation on a production aircraft to the original digital mock-up. *SAE International Journal of Aerospace*, 4:880–892, 2011.
- [14] A. W. Vieira, P. L. Drews, and M. F. Campos. Efficient change detection in 3d environment for autonomous surveillance robots based on implicit volume. In *Robotics and Automation (ICRA), 2012 IEEE International Conference on*, pages 2999–3004. IEEE, 2012.